

Meson-exchange-currents contribution to axial charge transitions

G. Barenboim and A. O. Gattone

*Departamento de Física, Comisión Nacional de Energía Atómica,
Avenida del Libertador 8250, 1429 Buenos Aires, Argentina*

E. D. Izquierdo

*Departamento de Física, FCEyN, Universidad de Buenos Aires,
Pabellón 1, Ciudad Universitaria, 1428 Buenos Aires, Argentina*

(Received 27 May 1993)

We study the contribution of meson-exchange currents (MEC) to axial charge transitions in the framework of quantum hadrodynamics II. We extend a previous work which considered the contributions of one-body processes and vacuum polarization corrections. Calculations in mean-field theory (the Walecka model) and in the relativistic Hartree approximation are presented. In each of these cases we show results using pseudovector and pseudoscalar πN coupling. We find that the MEC contribution to the process is always sizable (much more so when using pseudoscalar coupling), transition dependent, and very sensitive to the coupling at the $\rho\pi$ vertex.

PACS number(s): 23.40.Hc, 27.80.+w

In a recent paper [1], we presented a relativistic impulse approximation (RIA) calculation of first-forbidden β -decay (FFBD) rates as an attempt to understand the enhancement of axial charge transitions found by Warburton [2] in his analysis of nuclei in the $A=205-212$ region. Warburton's fit to 19 FFBD transitions in this region parametrized as $g_A^{\text{eff}} = g_A^{\text{free}}(1 + \delta_{\text{MEC}})$ gives a "best fit" value of $\delta_{\text{MEC}} = 1.01 \pm 0.05$, which is roughly 50% larger than the anticipated $\delta_{\text{MEC}} \approx 0.6$ as given by Kirchbach and Reinhardt [3]. In the calculations of Ref. [1] (hereafter I) we employed relativistic shell-model wave functions obtained in both (i) the mean-field (MF) approximation and (ii) the relativistic Hartree (RH) approximation (where the shift in the vacuum energy at finite baryon density is taken into account). Upon comparing the results obtained in I to a nonrelativistic IA calculation we found a substantial increment ($\approx 50\%$) in β -decay rates when working in the mean-field approximation and a smaller increase (around 30% depending somewhat on the case studied) when employing the relativistic Hartree wave functions. A calculation of random-phase-approximation- (RPA-) type vertex corrections (core polarization) was also conducted but found to give a vanishing contribution for the small momentum transfers involved in nuclear β decay.

The enhancement found in I was interpreted as originating on the *Born* and *pair* terms which are included naturally in a RIA calculation. In this situation, and

unlike the nonrelativistic case, a dramatic contribution from the two-body (2B) currents is not anticipated since a great deal of the enhancement shows up already at the IA level. In any event, in order to have a complete description of the axial-charge process from the relativistic point of view it is necessary to formulate the contribution of two-body currents within the same consistent framework. The aim of this paper is to present results of a relativistic meson-exchange-current (MEC) calculation of processes contributing to axial charge transitions. We shall give results for both the MF and the RH approximations for the transitions in Pb and Bi presented in I and we shall also compare with the IA results presented there (relativistic and nonrelativistic).

Further motivation for this work arises from the results of some recent calculations [4,5], involving the inclusion of heavy mesons and which have shown to provide a satisfactory explanation to the observed enhancement. Since this heavy-meson contribution arises naturally in relativistic hadron theories, it is important to find out what its predictions are and how they come about.

For consistency we use for the MEC calculation the same Lagrangian (quantum hadrodynamics II, QHD-II [6]) employed in I. It includes, besides the nucleon field, two isoscalar meson fields, the σ (scalar) and the ω (vector), and two charged isovector meson fields, the π (pseudoscalar) and the ρ (vector). The Lagrangian is renormalizable and is given by

$$\begin{aligned} \mathcal{L} = & \bar{\psi} [i\gamma_\mu D^\mu - (m_N - g_\sigma \sigma) - g_\omega \gamma_\mu \omega^\mu - ig_\pi \gamma_5 \boldsymbol{\tau} \cdot \boldsymbol{\pi}] \psi + g_\rho (\partial^\mu \boldsymbol{\pi} \times \boldsymbol{\pi}) \cdot \boldsymbol{\rho}_\mu + \frac{1}{2} g_\rho^2 (\boldsymbol{\pi} \times \boldsymbol{\rho}_\mu) \cdot (\boldsymbol{\pi} \times \boldsymbol{\rho}^\mu) \\ & + \frac{1}{2} (\partial_\mu \sigma \partial^\mu \sigma - m_\sigma^2 \sigma^2) - \frac{1}{4} F_{\mu\nu} F^{\mu\nu} + \frac{1}{2} m_\omega^2 \omega_\mu \omega^\mu - \frac{1}{4} \mathbf{B}_{\mu\nu} \mathbf{B}^{\mu\nu} + \frac{1}{2} m_\rho^2 \boldsymbol{\rho}_\mu \cdot \boldsymbol{\rho}^\mu \\ & + \frac{1}{2} (\partial_\mu \boldsymbol{\pi} \cdot \partial^\mu \boldsymbol{\pi} - m_\pi^2 \boldsymbol{\pi} \cdot \boldsymbol{\pi}) + \frac{1}{2} g_{\sigma\pi} m_\sigma \sigma \boldsymbol{\pi} \cdot \boldsymbol{\pi}. \end{aligned} \quad (1)$$

In Eq. (1) the neutral and charged vector meson field strengths are defined by

$$F^{\mu\nu} \equiv \partial^\mu \omega^\nu - \partial^\nu \omega^\mu, \quad (2a)$$

$$\mathbf{B}_{\mu\nu} \equiv \partial_\mu \boldsymbol{\rho}_\nu - \partial_\nu \boldsymbol{\rho}_\mu - g_\rho (\boldsymbol{\rho}_\mu \times \boldsymbol{\rho}_\nu), \quad (2b)$$

respectively, and we have also defined the covariant derivative

$$D_\mu \equiv \partial_\mu + i\frac{1}{2} g_\rho \boldsymbol{\tau} \cdot \boldsymbol{\rho}_\mu. \quad (2c)$$

There is a Higgs-meson sector associated with the ρ -

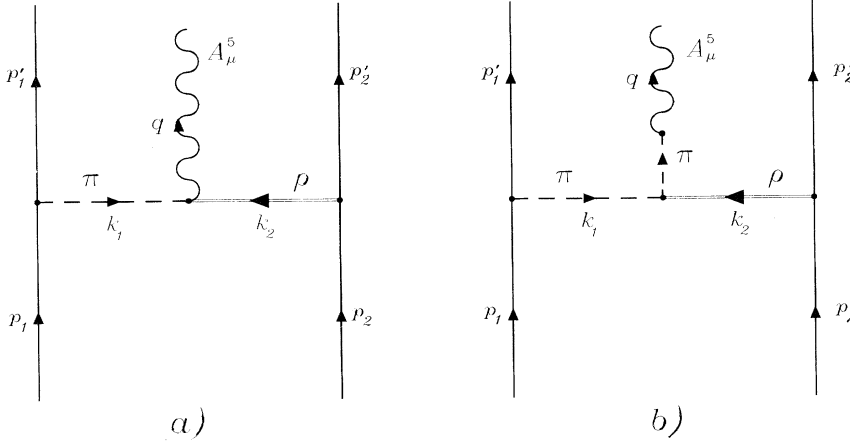


FIG. 1. Diagrams included in the two-body contribution to axial charge transitions: (a) $\rho\pi$ and (b) $\rho\pi\pi$. The external and internal momenta depicted in the figure are those employed in the actual calculations.

meson field which has been suppressed by taking the scalar Higgs mass to be very large.

At tree level the two-nucleon MEC operator is given by the sum of the two graphs shown in Fig. 1. They include the $\rho\pi$ term (a) and a pion-pole diagram ($\rho\pi\pi$) (b). These two graphs are the most important since they involve pion exchanges which generate the longest-range exchange currents. We have not considered the Δ contribution since, on the one hand, there is not yet an established form to include the Δ into QHD calculations, and on the other Nozawa *et al.* [7] have shown that its contribution to these processes is small.

The original QHD-II Lagrangian [as given in Ref. [6] and in Eq. (1)] uses pseudoscalar πN coupling in order to preserve renormalizability. To take care of the otherwise anomalous scattering length in πN scattering an additional interaction term between the σ and the π fields is included [last term in Eq. (1)]. In our calculations we found that the use of the pseudoscalar coupling produces large MEC contributions which are not canceled by the $\sigma\pi\pi$ term. In fact, the $\sigma\pi\pi$ contribution to the 2B current [a diagram similar to part (b) of Fig. 1 with the ρ -meson line replaced by a σ line] vanishes in the $q \rightarrow 0$ limit. It is known that in free space these cancellations are necessary because the nonderivative coupling $\bar{\psi}\gamma_5\tau\cdot\pi\psi$ does not contain *per se* the soft-pion limit [8]. On the other hand, it is also known that the cancellations

are difficult to maintain in the many-body problem, as we find in our case. Therefore, we have performed calculations using (1) but substituting pseudovector coupling for the original pseudoscalar πN interaction and dropping the $\sigma\pi\pi$ term altogether. We want to remark that either coupling has the correct low-energy limit in the two-body case and that the partially conserved axial-current (PCAC) results on two nucleons do not depend on which one is chosen.

Renormalizability is lost when working with pseudovector coupling. This poses, however, no major obstacle for comparing with the results in I since for either πN coupling the MF and the RH approaches cancel the π contribution by parity considerations. Regarding the RPA-type vertex corrections also presented in I, their vanishing contributions turn out to be independent of the coupling used at the πN vertex.

Use of the Feynman rules with vertices and propagators from the Lagrangian (1) (with pseudovector coupling and no $\sigma\pi\pi$ term) gives rise to an expression for the two-body $\rho\pi$ and $\rho\pi\pi$ currents of the form

$$J_5^{\mu,c}(\rho\pi; q, k_1, k_2) = -i\frac{g_\pi g_\rho}{4M} [\tau_1 \times \tau_2]^c \bar{u}(p'_1)\gamma^5 k_1 u(p_1) \times \frac{1}{k_1^2 - m_\pi^2} \Gamma^{\mu\nu} \frac{g_{\nu\eta}}{k_2^2 - m_\rho^2} \bar{u}(p'_2)\gamma^\eta u(p_2), \quad (3a)$$

$$J_5^{\mu,c}(\rho\pi\pi; q, k_1, k_2) = -i\frac{g_\pi g_\rho^2}{4M} [\tau_1 \times \tau_2]^c \bar{u}(p'_1)\gamma^5 k_1 u(p_1) f_\pi \frac{q^\mu}{q^2 - m_\pi^2} \frac{1}{k_1^2 - m_\pi^2} \frac{g'_\eta}{k_2^2 - m_\rho^2} (q + k_1)_\nu \bar{u}(p'_2)\gamma^\eta u(p_2). \quad (3b)$$

In the last equation we used, for the weak-pion vertex,

$$\langle 0 | J_\mu^{5,a}(0) | \pi^b(q) \rangle = i f_\pi q_\mu \delta^{ab}, \quad (4)$$

with $f_\pi = 0.93$ GeV the pion-decay constant.

In Eq. (3a), the (isospin-independent) tensor $T_{\mu\nu}$ is such that

$$\epsilon^{abc} T_{\mu\nu} = \langle \pi^b(k_1) | J_\mu^{5,a}(q) | \rho_\mu^c(k_2) \rangle \quad (5)$$

and its value is determined uniquely from the PCAC constraint. To show this we first notice that the π -absorption amplitude on two nucleons (obtained from the $\rho\pi\pi$ diagram by removing the external A_μ^5 line) reads

$$M^c(2B) = -(g_\pi g_\rho^2/4M) [\tau_1 \times \tau_2]^c \bar{u}(p'_1)\gamma^5 k_1 u(p_1) \times \frac{1}{k_1^2 - m_\pi^2} \frac{g'_\eta}{k_2^2 - m_\rho^2} (q + k_1)_\nu \bar{u}(p'_2)\gamma^\eta u(p_2). \quad (6)$$

On the other hand, the $(-i)\times 4$ divergence of the full 2B current is given by

TABLE I. Parameters used for the calculations presented in the text.

	$g_{\sigma N}^2$	m_σ	$g_{\omega N}^2$	g_π^2	g_ρ^2	M^*/M
MFT	109.6	520	190.4	178.4	65.23	0.54
RHA	54.3	458	102.8	178.4	65.23	0.73

TABLE II. Results for the $\nu : 2g_{9/2} \rightarrow \pi : 1h_{9/2}$ transition in $^{209}\text{Pb} \rightarrow ^{209}\text{Bi}$. First row: the nonrelativistic (NRIA) and the relativistic (RIA) impulse approximation results are from I. The meson-exchange-current results are from this paper. The table includes results for the mean-field (MFT) and the relativistic Hartree (RHA) calculations. Meson-exchange-current results are shown for pseudovector [MEC(PV)] and pseudoscalar [MEC(PS)] couplings. Second row: enhancement with respect to the NRIA.

NRIA	MFT			RHA		
	RIA	MEC(PV)	MEC(PS)	RIA	MEC(PV)	MEC(PS)
-1.23×10^{-1}	-1.98×10^{-1}	-1.14×10^{-1}	-2.63×10^{-1}	-1.57×10^{-1}	-8.97×10^{-2}	-2.14×10^{-1}
	0.60	0.90	2.14	0.28	0.72	1.72

$$q_\mu J_5^{\mu,c}(\rho\pi + \rho\pi\pi) = -i(g_\pi g_\rho / 4M)[\boldsymbol{\tau}_1 \times \boldsymbol{\tau}_2]^c \bar{u}(p'_1)\gamma^5 k_1 u(p_1) \\ \times \frac{1}{k_1^2 - m_\pi^2} \frac{1}{k_2^2 - m_\rho^2} \left\{ q_\mu \Gamma^{\mu\eta} + g_\rho f_\pi \frac{q^2}{q^2 - m_\pi^2} (q + k_1)_\eta \right\} \bar{u}(p'_2)\gamma^\eta u(p_2). \quad (7)$$

The PCAC relation on two nucleons requires that

$$q_\mu J_5^{\mu,c} = i f_\pi [m_\pi^2 / (q^2 - m_\pi^2)] M^c(2B), \quad (8)$$

and this is satisfied if

$$q_\mu \frac{\Gamma^{\mu\eta}}{f_\pi g_\rho} (q^2 - m_\pi^2) + q^2 (q + k_1)_\eta = m_\pi^2 (q + k_1)_\eta. \quad (9)$$

A solution can be found when

$$\Gamma^{\mu\eta} = -f_\pi g_\rho [g^{\mu\eta} + q^\mu k_1^\eta / (q^2 - m_\pi^2)], \quad (10)$$

which gives the strength at the $\pi A\rho$ vertex. Notice that in the soft-pion limit ($k_1 \rightarrow 0$), $\Gamma^{\mu\eta} = -f_\pi g_\rho g^{\mu\eta}$ which is the same strength obtained by Ivanov and Truhlik [9] in the soft-pion limit of their hard-pion model. From the above it is clear then that the Lagrangian (1) satisfies PCAC on two nucleons and has the correct behavior in the soft-pion limit.

To study individual transitions it is convenient to perform a multipole decomposition of the current matrix elements. For the cases analyzed in I, and pursued in this work, the main contributions come from the Coulomb operator

$$C_{JM}^{(5)}(q) = \int d^3r M_J^M(q\mathbf{r}) J_0^5(\mathbf{r}), \quad (11)$$

where

$$M_J^M(q\mathbf{r}) = j_J(qr) Y_J^M(\hat{\mathbf{r}}). \quad (12)$$

For the small momentum transfers involved in FFBD's the $J = 0$ multipole is the most important. The two-body matrix element contributing to axial charge transitions may be written in the form

$$\langle J_1 || \hat{C}_0^{(2)}(q \rightarrow 0) || J_2 \rangle = \sum_{a,b} \sum_{a',b'} \langle (a', b') j_f || C_0^{(5)} || (a, b) j_i \rangle \\ \times \Psi_{J=0}^{(1,2)}((a', b') j_f, (a, b) j_i), \quad (13)$$

TABLE III. Results for the $\pi : (3s_{1/2})^{-1} \rightarrow \nu : 3p_{1/2}^{-1}$ transition in $^{207}\text{Tl} \rightarrow ^{207}\text{Pb}$. First row: the nonrelativistic (NRIA) and the relativistic (RIA) impulse approximation results are from I. The meson-exchange-current results are from this paper. The table includes results for the mean-field (MFT) and the relativistic Hartree (RHA) calculations. Meson-exchange-current results are presented for pseudovector [MEC(PV)] and pseudoscalar [MEC(PS)] couplings. Second row: enhancement with respect to the NRIA.

NRIA	MFT			RHA		
	RIA	MEC(PV)	MEC(PS)	RIA	MEC(PV)	MEC(PS)
8.30×10^{-2}	1.16×10^{-1}	4.57×10^{-2}	7.66×10^{-2}	9.13×10^{-2}	4.03×10^{-2}	6.42×10^{-2}
	0.39	0.55	0.92	0.17	0.43	0.70

where $\Psi_{J=0}^{(1,2)}((a', b') j_f, (a, b) j_i)$ are the two-body density-matrix elements defined in terms of the particle operators, c_α , by

$$\langle J_1 || \Psi_{J=0}^{(1,2)} || J_2 \rangle = \left\langle J_1 \left\| \frac{1}{[J]} \left[[c_{a'}^\dagger \otimes c_{b'}^\dagger]_{j_f} \otimes [\tilde{c}_a \otimes \tilde{c}_b]_{j_i} \right]_J \right\| J_2 \right\rangle, \quad (14)$$

with $\tilde{c}_\alpha = (-1)^{j-m_j} c_{-\alpha}$. The sums run over all possible initial pairs of relativistic single-particle states (a, b) leading to all possible final pairs of relativistic single-particle states (a', b') . Substituting (11) into (13), using Eqs. (3), and carrying out the summations one obtains the results that we show shortly. Numerical details about the calculation of the two-body matrix element of (13) will be given elsewhere [10].

The coupling constants used in the calculations are shown in Table I. Both sets of parameters, MFT and RHA, are from Ref. [11] and are not tuned specifically to the lead region. The scalar masses were determined by fitting the charge radius of ^{40}Ca . The other masses, fixed to their experimental values, are $M = 939$ MeV, $m_\omega = 783$ MeV, $m_\rho = 770$ MeV, and $m_\pi = 139$ MeV. In the calculations we used for g_ρ^2 the value determined by fitting the bulk symmetry energy in infinite matter, $a_4 = 35$ MeV. Results obtained using g_ρ^2 determined from the $\rho \rightarrow \pi\pi$ decay will also be shown. The intrinsic structure of the nucleons was considered via an additional q^2 dependence of the form $(1 + q^2/M_A^2)^{-2}$ with $M_A = 1.2$ GeV.

In Tables II and III we summarize our results for the two transitions we considered: the $\nu : 2g_{9/2} \rightarrow \pi : 1h_{9/2}$ transition in $^{209}\text{Pb} \rightarrow ^{209}\text{Bi}$ and the $\pi : (3s_{1/2})^{-1} \rightarrow \nu :$

TABLE IV. Full increment ($\delta_{\text{MEC}} = \text{RIA} + \text{MEC}$) for the transitions in Tables II and III using $g_\rho^2 = 65.23$.

$\delta_{\text{MEC}} = \text{RIA} + \text{MEC}$	MFT		RHA	
	MEC(PV)	MEC(PS)	MEC(PV)	MEC(PS)
$^{209}\text{Pb} \rightarrow ^{209}\text{Bi}$	1.53	2.74	1.00	2.00
$^{207}\text{Tl} \rightarrow ^{207}\text{Pb}$	0.94	1.31	0.60	0.87

($3p_{1/2}^{-1}$) transition in $^{207}\text{Tl} \rightarrow ^{207}\text{Pb}$. The nonrelativistic impulse approximation (NRIA) results are from I. We divided the tables into two sets, one for the mean-field (MFT) and the other for the relativistic Hartree (RHA) calculations. For each set we quote results for the impulse approximation (RIA) and for the meson-exchange-current calculation. The latter are given in pseudovector [MEC(PV)] and in pseudoscalar [MEC(PS)] couplings. The second row of the tables shows the increase with respect to the NRIA for the entries in the first row.

In Table IV we show results for δ_{MEC} which was redefined to contain the sum of the RIA plus the MEC increments. This is in line with the fact that part of the enhancement has already been considered in the RIA calculation. The results are presented for the two transitions. Comparing the MFT with the RHA calculations we notice that the first one is consistently larger than the second for either transition, pointing out the role played by the vacuum in relativistic calculations. In PV coupling the MFT results for the transition in Pb give a 153% enhancement with respect to the NRIA, as compared to 100% for the RHA. In Tl the enhancement decreases from 94% (MFT) to 60% (RHA). This is consistent with the fact that in RHA the ratio M^*/M is closer to one as can be seen from Table I.

One point to notice is the difference between results obtained using pseudovector and pseudoscalar coupling, the latter being consistently larger. Because pseudovector coupling shows the correct low-energy behavior in the many-body problem it is has been considered [8] as the appropriate coupling to be used in finite nuclei calculations. In this case, we may conclude that in QHD the enhancement observed in the lead region (1) shows up strongly in both the MFT and RHA, (2) the strength depends on the particular transition studied, and (3) in the RHA it is 40–50% smaller than in the MFT.

Despite these conclusions we call attention to the dependence of the results on the value of g_ρ^2 . Calculations in finite nuclei within QHD (see, for example, Refs. [6]

TABLE V. Same as Table IV but using $g_\rho^2 = 36.76$.

$\delta_{\text{MEC}} = \text{RIA} + \text{MEC}$	MFT		RHA	
	MEC(PV)	MEC(PS)	MEC(PV)	MEC(PS)
$^{209}\text{Pb} \rightarrow ^{209}\text{Bi}$	0.87	1.81	0.47	1.22
$^{207}\text{Tl} \rightarrow ^{207}\text{Pb}$	0.55	0.92	0.29	0.55

and [12]) usually employ g_ρ^2 determined from the fitting to the symmetry energy instead of the coupling determined from the decay of the ρ meson. The first is a many-body argument which favors its use over the second. The largest ρ coupling, however, besides violating the Kawarabayashi-Suzuki-Riazuddin-Fayyazuddin relation [13], seems to provide too much enhancement for the transition in lead. Since there are not strong enough arguments to discriminate them, and given the sensitivity of the results to either choice, we include in Table V results for δ_{MEC} using $g_\rho^2 = 36.76$. With this coupling MFT with PV coupling seems to account for the observed enhancement whereas the RHA leaves room for the presence of other effects. We emphasize the necessity for consistency in the use of the same coupling when determining the nuclear wave functions and when calculating the matrix element (13). One point to mention is that the RIA results do not depend on the ρ coupling constant.

Summarizing, we have studied the contribution of MEC processes to axial charge transitions for nuclei in the lead region. We have thus extended the work of Ref. [1] which, within the same relativistic theory (QHD-II), considered the contributions of one-body processes and vacuum polarization corrections. We conducted calculations in mean-field theory (the Walecka model) and in the relativistic Hartree approximation where the full one-nucleon-loop effects are considered. In each of these cases we presented results using pseudovector and pseudoscalar πN couplings. We found that the MEC contribution to the process is always sizable (much more so when using pseudoscalar coupling), transition dependent, and very sensitive to the coupling at the $\rho\pi$ vertex (which is also twice the coupling at the ρNN vertex by gauge invariance). The RHA approach consistently gives results which are 40% smaller than in the MFT. Further studies of other transitions in the periodic table are necessary to establish the mass dependence of the effect. Also it is necessary to further constrain the range of the ρ -meson coupling constant to eliminate ambiguities in the interpretation of the results.

- [1] A. O. Gattone, E. D. Izquierdo, and M. Chiapparini, Phys. Rev. C **46**, 788 (1992).
- [2] E. K. Warburton, Phys. Rev. Lett. **66**, 1823 (1991); Phys. Rev. C **44**, 233 (1991).
- [3] M. Kirchbach and H. Reinhardt, Phys. Lett. B **208**, 79 (1988).
- [4] I. S. Towner, Nucl. Phys. **A542**, 631 (1992).
- [5] M. Kirchbach, D. O. Riska, and K. Tsushima, Nucl. Phys. **A542**, 616 (1992).
- [6] B. D. Serot and J. D. Walecka, in *The Relativistic Nuclear Many-Body Problem*, Advances in Nuclear Physics Vol. 16, edited by J. W. Negele and E. Vogt (Plenum Press, New York, 1986).
- [7] S. Nozawa, K. Kubodera, and H. Ohtsubo, Nucl. Phys.

- A453**, 645 (1986).
- [8] B. D. Serot, Rep. Prog. Phys. **11**, 1855 (1992).
- [9] E. Ivanov and E. Truhlik, Nucl. Phys. **A316**, 437 (1979).
- [10] E. D. Izquierdo, A. O. Gattone, and G. Barenboim (unpublished).
- [11] C. J. Horowitz and B. D. Serot, Phys. Lett. **140B**, 181 (1984).
- [12] R. J. Furnstahl and C. E. Price, Phys. Rev. C **41**, 1792 (1990). The same authors use this value to calculate density distributions in *ibid.* **44**, 895 (1991), and a slightly larger one ($g_\rho^2 = 83.30$) in *ibid.* **40**, 1398 (1989).
- [13] K. Kawarabayashi and M. Suzuki, Phys. Rev. Lett. **16**, 255 (1966); Riazuddin and Fayyazuddin, Phys. Rev. **147**, 1071 (1966).